



Mast cell chymase limits the cardiac efficacy of Ang I–converting enzyme inhibitor therapy in rodents

Chih-Chang Wei,^{1,2} Naoki Hase,³ Yukiko Inoue,⁴ Eddie W. Bradley,¹ Eiji Yahiro,⁵ Ming Li,⁵ Nawazish Naqvi,⁵ Pamela C. Powell,^{1,2} Ke Shi,¹ Yoshimasa Takahashi,³ Keiji Saku,⁶ Hidenori Urata,⁴ Louis J. Dell’Italia,^{1,2,7} and Ahsan Husain⁵

¹Department of Medicine, University of Alabama at Birmingham. ²VA Medical Center, Birmingham, Alabama. ³Teijin Institute for Bio-medical Research, Teijin Pharma Ltd., Tokyo, Japan. ⁴Department of Cardiovascular Diseases, Fukuoka University Chikushi Hospital, Fukuoka, Japan. ⁵Division of Cardiology, Department of Medicine, Emory University, Atlanta, Georgia. ⁶Department of Cardiology, Fukuoka University School of Medicine, Fukuoka, Japan. ⁷Department of Physiology and Biophysics, University of Alabama at Birmingham.

Ang I–converting enzyme (ACE) inhibitors are widely believed to suppress the deleterious cardiac effects of Ang II by inhibiting locally generated Ang II. However, the recent demonstration that chymase, an Ang II–forming enzyme stored in mast cell granules, is present in the heart has added uncertainty to this view. As discussed here, using microdialysis probes tethered to the heart of conscious mice, we have shown that chronic ACE inhibitor treatment did not suppress Ang II levels in the LV interstitial fluid (ISF) despite marked inhibition of ACE. However, chronic ACE inhibition caused a marked bradykinin/B2 receptor–mediated increase in LV ISF chymase activity that was not observed in mast cell–deficient *Kit^W/Kit^{W-v}* mice. In chronic ACE inhibitor–treated mast cell–sufficient littermates, chymase inhibition decreased LV ISF Ang II levels substantially, indicating the importance of mast cell chymase in regulating cardiac Ang II levels. Chymase-dependent processing of other regulatory peptides also promotes inflammation and tissue remodeling. We found that combined chymase and ACE inhibition, relative to ACE inhibition alone, improved LV function, decreased adverse cardiac remodeling, and improved survival after myocardial infarction in hamsters. These results suggest that chymase inhibitors could be a useful addition to ACE inhibitor therapy in the treatment of heart failure.

Introduction

Ang I–converting enzyme (ACE), a membrane-bound zinc metallo-peptidase, converts the prohormone Ang I to Ang II and inactivates bradykinin (1). Many large, prospective, randomized clinical trials over the last 20 years have shown the usefulness of ACE inhibitors in reducing overall mortality in patients with myocardial infarction (MI) and various degrees of LV systolic dysfunction (2–4). Although the mechanisms underlying these beneficial effects are not fully understood, suppression of Ang II in the heart and an improved hemodynamic state are thought to be important. The identification of an ACE-independent mast cell (MC) pathway for Ang II generation in the human heart raised the possibility that chronic ACE inhibitor therapy may not completely suppress Ang II (5–7), which may in turn cause adverse LV remodeling by activating Ang II receptor subtypes 1 (AT₁ receptor) and 2 (AT₂ receptor) (8, 9).

Chymase, an efficient Ang II–forming serine protease (6), is mainly found in MCs. In the human heart, it is also found in the cardiac interstitial space and in some cardiac ECs (10). Chymases have also been reported in cultured neonatal rat ventricular cardiomyocytes (11) and rat VSMCs (12). EM-immunohistochemical studies using human heart tissue indicate that the positively charged chymase molecule is associated with the matrix within the cardiac interstitial fluid (ISF) space (10). This localization suggests a role for chymase in interstitial Ang II formation, as does the find-

ing that, in anesthetized dogs, Ang II levels in the cardiac ISF are not suppressed by acute ACE inhibitor administration (13). These studies also indicate the presence of a functional chymase-dependent Ang II–forming pathway in the heart. However, studies with conscious baboons questioned this notion. For example, using direct coronary artery infusions of [Pro¹¹, Dala¹²]Ang I, a substrate that is converted to Ang II by chymase but not ACE, Hoit et al. (14) were unable to demonstrate a change in cardiac function, despite the fact that the non-ACE–dependent Ang II–forming activity is higher than ACE-dependent Ang II–forming activity in baboon heart homogenates. Because chymase is activated and stored in secretory granules, the possibility exists that chymase activity in tissue homogenates does not reflect extracellular chymase activity in the hearts of conscious animals, which could be minimal. Its interstitial localization in histological tissue sections may be exaggerated because nonfailing human hearts used to study its localization were obtained from victims of accidents, who were subjected to a number of drugs that could lead to chymase release, including anesthetics. Moreover, protease inhibitors present in ISF obtained from skin blisters have been shown to inhibit chymase activity (15). If these inhibitors occur in the cardiac interstitium, they could ensure that chymase remains constitutively inactivated. In addition, the identification of distinct enzymes from other cell types, such as cathepsin G from neutrophils (16), which can also form Ang II, makes the importance of MC-mediated Ang II formation in the heart uncertain.

Chronic ACE inhibitor treatment influences plasma Ang II levels in a biphasic manner (17, 18). The immediate response is a marked fall in plasma Ang II levels. But over time, plasma Ang II levels

Authorship note: Chih-Chang Wei, Naoki Hase, and Yukiko Inoue contributed equally to this work.

Conflict of interest: The authors have declared that no conflict of interest exists.

Citation for this article: *J Clin Invest.* 2010;120(4):1229–1239. doi:10.1172/JCI39345.

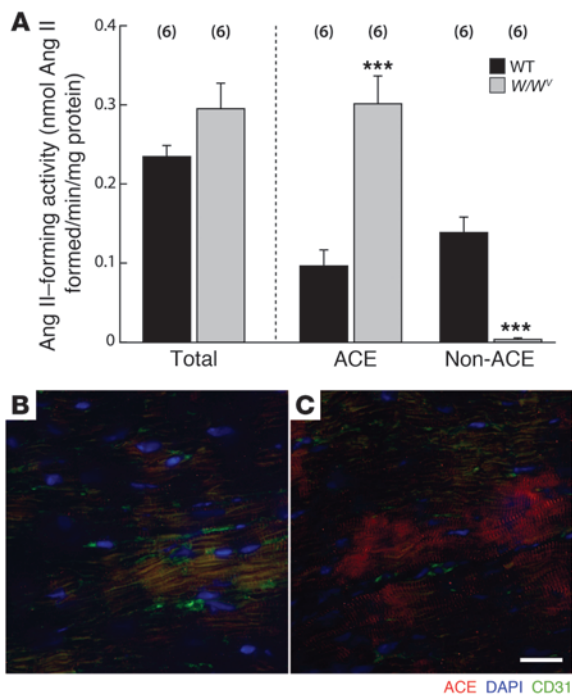


Figure 1

ACE and non-ACE Ang II-forming activities and ACE immunoreactivity in WT and W/W^v LV homogenates (**A**). Values are mean ± SEM. In each group, n = 6. All measurements were made in 7-week-old mice. Ang II-forming activity: total, which was determined in the absence of any inhibitors; ACE, that level of the total that was inhibited by the ACE inhibitor lisinopril (10 μM); and non-ACE, the total minus the ACE activity. ***P < 0.001. Photomicrographs showing ACE immunoreactivity in (**B**) WT and (**C**) W/W^v LV tissue sections. ACE (red); CD31, which identifies ECs (green); and DAPI, which identifies nuclei (blue). Note ACE immunoreactivity in clusters of cardiomyocytes in the W/W^v LV tissue section (**C**) but not in WT LV section (**B**). ACE immunoreactivity was only weakly associated with CD31-positive ECs. Scale bar: 20 μm.

return to near normal levels despite substantial ACE inhibition. Because ACE is also a kininase, tissue and plasma bradykinin levels are markedly elevated during chronic ACE inhibitor treatment (1). Here we report that cardiac ACE inhibition produces a bradykinin-independent release of chymase from MCs in conscious mice, which maintains cardiac ISF Ang II levels. These studies not only demonstrate the in vivo functionality of the cardiac non-ACE pathway but also show that it originates from MCs. Our findings challenge the notion that the cardiac efficacy of ACE inhibitors requires Ang II suppression in the heart. We also show that, in animals treated with an ACE inhibitor, chymase inhibition improves LV function and decreases adverse cardiac remodeling after MI.

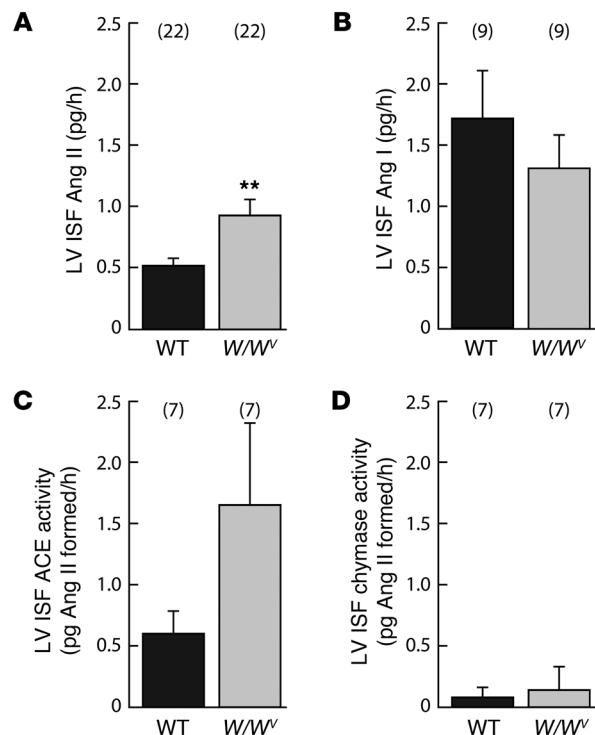
Results

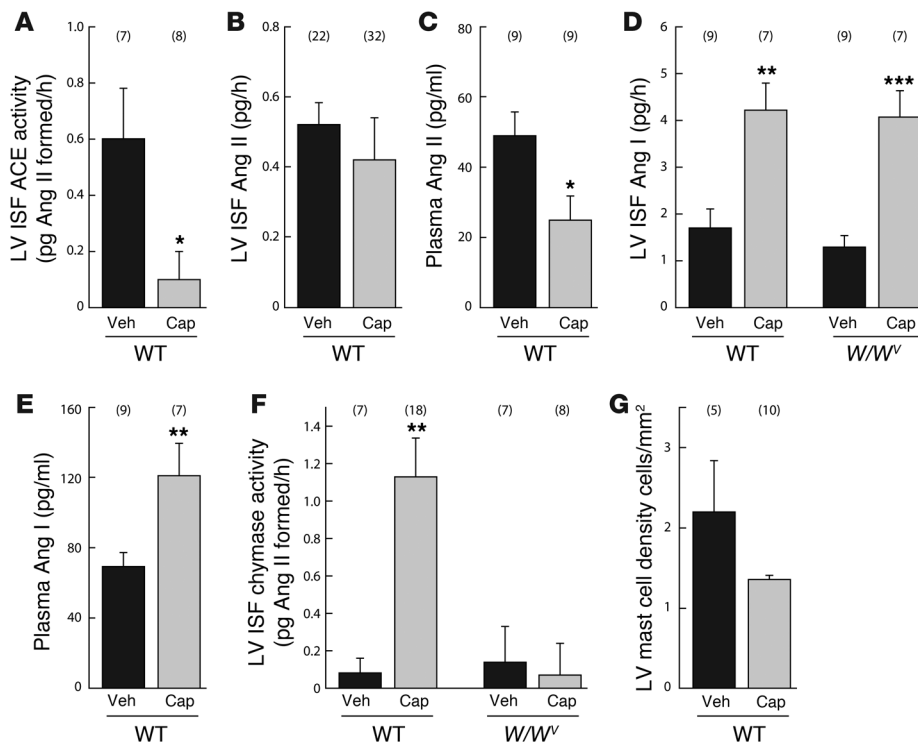
MCs are the major source of the non-ACE Ang II-forming activity in LV homogenates. We observed similar levels of ACE (ACE inhibitor-sensitive Ang II-forming activity) and non-ACE (ACE inhibitor-resistant Ang II-forming activity) Ang II-forming activities in mouse LV homogenates (Figure 1A). The mouse heart, thus, has the potential to regulate Ang II locally through these 2 pathways. One source of the non-ACE activity is the MC, which elaborates chymase (16). To evaluate this, we studied the effect of MC deficiency on non-ACE activity in LV homogenates. LV non-ACE activity was reduced by more than 95% (P < 0.001) in MC-deficient *Kit^W/Kit^{W-v}* (W/W^v) mice (19), relative to MC-sufficient WT littermates (Figure 1A), implicat-

Figure 2

Basal Ang II (**A**), Ang I (**B**), ACE activity (**C**), and chymase activity (**D**) in the LV ISF of conscious WT and W/W^v mice. In vivo microdialysis was used to collect samples for these measurements. In addition, using this procedure, [Pro¹⁰]Ang I and [Pro¹¹,DAla¹²]Ang I conversion to Ang II in the LV ISF was used to measure ACE- and chymase-like activities, respectively. Values are mean ± SEM. In each group, values in parentheses represent n. **P < 0.01.

ing MCs as the major source of LV non-ACE activity. Interestingly, total LV homogenate Ang II-forming activity in W/W^v mice was not different from that in WT mice because of a 3-fold increase in W/W^v LV ACE activity (Figure 1A). Quantitative immunofluorescence showed a 2.6-fold higher ACE immunoreactivity in W/W^v LV tissue sections relative to WT (23 ± 7.6 versus 59 ± 4.4 AU/μm² in WT and W/W^v LVs, respectively; n = 5/group; P < 0.01) (Figure 1, B and C); in W/W^v mice, ACE immunoreactivity was mainly associated with cardiomyocytes (Figure 1C). However, ACE mRNA levels in isolated W/W^v cardiomyocytes were similar to those in WT cardiomyocytes (0.066 ± 0.009 versus 0.0512 ± 0.003 ACE/GAPDH mRNA transcript ratio in WT and W/W^v, respectively; n = 6–7 cardiomyocyte isolations/group). It is tempting to speculate that decreased shedding of cell surface ACE, which may be regulated by ACE secretase (20), rather than increased transcription, produced higher ACE levels in W/W^v LVs; however, this increase is unlikely to be due to suppressed chymase-dependent Ang II formation because, in WT mice, chronic inhibition of mouse MC protease-4 (MMCP4), the major Ang II-forming chymase in the LV (see below), did not increase LV ACE immunoreactivity (data not shown).



**Figure 3**

Effect of chronic ACE inhibitor treatment on angiotensins and Ang II-forming enzyme activities in conscious mice. Effect of chronic captopril treatment (150 mg captopril/kg/d; for 2 weeks) on (A) LV ISF ACE activity, (B) LV ISF, (C) plasma Ang II, (E) plasma Ang I, and (G) MC density in WT mice. Effect of chronic captopril treatment on (D) LV ISF Ang I and (F) LV ISF chymase activity in WT and *W/W^v* mice. Values are mean ± SEM. In each group, values in parentheses represent *n*. **P* < 0.05; ***P* < 0.01; ****P* < 0.001. Veh, vehicle; Cap, captopril.

In the basal state, cardiac, chymase-like activity is not in the ISF sub-compartment. Steady-state ISF Ang I/Ang II ratios in the LV of conscious mice, as measured by in vivo microdialysis, were greater than 1 (approximately 3.6) (Figure 2, A and B), suggesting that the rate-limiting step in Ang II generation in the LV ISF is Ang I activation. Next, we estimated ACE- and chymase-like Ang II-forming activities in the LV ISF of conscious mice. We used [Pro¹⁰]Ang I and [Pro¹¹,DAla¹²]Ang I conversion to Ang II in the LV ISF as a measure of ACE- and chymase-like activities, respectively. While [Pro¹⁰]Ang I is converted to Ang II by ACE, but not chymase (21), [Pro¹¹,DAla¹²]Ang I is converted to Ang II by chymase, but not ACE (14, 22). These selective substrates were delivered in the lumen of the microdialysis probe in vivo. Increase in Ang II over baseline in the microdialysis probe retentate (which involves the diffusion of Ang II, generated from these substrates by ISF enzymes, from the ISF to the lumen of the microdialysis probe) during the infusion of [Pro¹⁰]Ang I or [Pro¹¹,DAla¹²]Ang I was taken to represent in vivo LV interstitial ACE- and chymase-like activities, respectively. In conscious WT mice, LV ISF ACE- and chymase-like activities were 0.6 and 0.08 pg Ang II formed/h, respectively (Figure 2, C and D), which indicates that ACE is the dominant Ang II-forming activity in the LV ISF. Moreover, LV ISF chymase-like activity in conscious WT mice was similar to that in *W/W^v* mice (Figure 2D), which, because they are deficient in cardiac chymase-like activity (Figure 1A), suggests that under basal conditions, chymase in the LV is not located extracellularly. But in *W/W^v* mice, LV ISF Ang II levels were 1.8-fold higher than in WT mice (*P* < 0.01; Figure 2A), which was associated with a 3-fold increase in LV tissue ACE activity (*P* < 0.001; Figure 1A) and a trend toward an increase in LV ISF ACE activity (Figure 2C). This association and low chymase-like activity in the LV ISF of conscious WT and *W/W^v* mice suggest a dominant role for local ACE in regulating LV ISF Ang II levels.

Chronic ACE inhibition causes chymase release into the LV ISF from MCs. To directly test the importance of ACE in regulating interstitial Ang II, we examined the effect of chronic (2 weeks) oral ACE inhibitor treatment (150 mg captopril/kg/d) on LV ISF Ang II. We took measurements of Ang II that enters the microdialysis probe per hour to directly reflect the level of Ang II in the LV ISF of the conscious mouse, realizing, of course, that factors such as peptide transfer rates in vivo are difficult to model based on idealized transfer rates determined in in vitro experiments with microdialysis probes. Chronic oral ACE inhibition with captopril produced an 85% decrease in LV ISF ACE activity (*P* < 0.05) in WT mice (Figure 3A), but it did not significantly lower ISF Ang II compared with vehicle controls (Figure 3B). In contrast, plasma Ang II levels decreased by approximately 2-fold (*P* < 0.05) after chronic ACE inhibition (Figure 3C). This was despite the fact that LV ISF and plasma Ang I levels increased by about 2-fold (*P* < 0.01) in both compartments (Figure 3, D and E). These findings could be interpreted in a number of ways. First, in the setting of chronic ACE inhibition, chymase, rather than ACE, is the major Ang II-forming enzyme in the LV ISF. Second, the rate of uptake of Ang II from the plasma, rather than the plasma Ang II concentration, is the chief determinant of LV ISF Ang II.

In the absence of a known mechanism for actively importing Ang II to the LV ISF, we considered the role of chymase and MCs in regulating LV ISF Ang II. Chronic ACE inhibition produced a 14-fold increase in LV ISF chymase-like activity (Figure 3F) (*P* < 0.01) and increased LV MMCP4 mRNA levels by approximately 10-fold (0.0034 ± 0.00023 versus 0.036 ± 0.008 MMCP4/GAPDH mRNA transcript ratio in vehicle- and captopril-treated WT mice, respectively; *n* = 5/group; *P* < 0.05). A time-course analysis indicated that LV ISF chymase activity increased as early as 24 hours after captopril administration, but at no time point were LV ISF Ang II levels suppressed by ACE inhibition (Supplemental Table 1; sup-

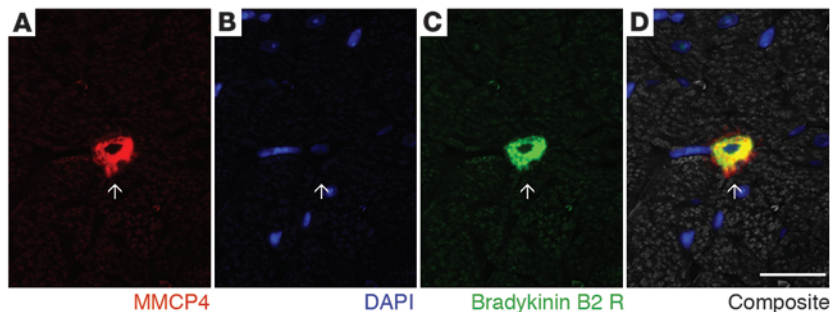


Figure 4
Bradykinin B2 receptors in LV MMCP4⁺ MCs. Photomicrographs of a LV section from an 8-week-old WT mouse stained for (A) MMCP4 to identify MC, (B) DAPI to detect nuclei, (C) and the B2 kinin receptor as well as the (D) composite image. Arrows show the location of the MMCP4⁺ MC. Scale bar: 20 μm.

plemental material available online with this article; doi:10.1172/JCI39345DS1). We also found that basal LV ISF chymase activity in MC-deficient *W/W^v* mice was low and similar to that observed in MC-sufficient WT mice, but the chronic ACE inhibitor-dependent 14-fold increase ($P < 0.01$) in this activity seen in WT mice was not observed in *W/W^v* mice (Figure 3F). This suggests that MCs are the main source of the chymase-like activity that is released into the LV ISF during chronic ACE inhibition.

Chronic ACE inhibition increased LV ISF Ang I levels in WT mice (Figure 3D). Because cardiac interstitial MCs elaborate renin (23), it is possible that this increase is produced by MC renin release. We tested this by comparing LV ISF Ang I levels, basal and after chronic ACE inhibition, in WT and *W/W^v* mice. We found that both basal and ACE inhibitor-induced LV ISF Ang I levels were not different between WT and *W/W^v* mice (Figure 3D), which does not support a role for MC renin in regulating LV ISF Ang I in the setting of ACE inhibition.

Bradykinin mediates chymase release into the LV ISF during chronic ACE inhibition. ACE inhibition prevents bradykinin degradation, and in rats, it increases LV ISF bradykinin levels (24). Because bradykinin elicits an inflammatory response (25), we evaluated the role of bradykinin/kinin B2 receptor activation on MC chymase release. We found that kinin B2 receptors are localized on MMCP4-positive MCs (Figure 4) — MMCP4 is the major Ang II-forming chymase in the LV (see below) — and the kinin B2 receptor antagonist Hoe-140 prevented the 14-fold increase LV ISF chymase-like activity in conscious WT mice caused by chronic ACE inhibition (Figure 5A). This indicates that chymase release into the LV ISF produced by ACE inhibition requires kinin B2 receptor activation and implies that bradykinin degranulates MCs.

We studied the *in vivo* effect of bradykinin on LV MC degranulation. MC numbers in LV sections were quantified using Giemsa (30–40 ×20 LV fields/mouse), which specifically stains MC granules. When MCs fully degranulate, Giemsa cannot visualize them. This and the difficulty with recognizing a partially degranulated MC have led some investigators to measure apparent MC loss as an estimate of degranulation (26). 24-hour microdialysis-based infusion of 5 ng/ml bradykinin decreased the number of identifiable LV MCs by 35% (0.38 ± 0.05 and 0.59 ± 0.08 MCs/mm²

in the bradykinin and vehicle groups, respectively; $n = 5$ /group; $P < 0.05$); 7-day pretreatment with 0.5 mg/kg/d Hoe-140 prevented this decrease (0.67 ± 0.06 MCs/mm², $n = 5$). Together with kinin B2 receptor localization on MCs (Figure 4, A–D), our findings suggest the possibility that bradykinin/kinin B2 receptors mediate MC degranulation in the LV of the conscious mouse. A 10-fold increase in MMCP4 mRNA levels in the LV (see above) coupled with a decrease in the number of identifiable MCs in WT LV after chronic ACE inhibitor treatment support this notion, although this latter change failed to reach significance (Figure 3G). We then tested to determine whether LV ISF Ang II formation in ACE-inhibited mice also requires kinin B2 receptor activation and found that

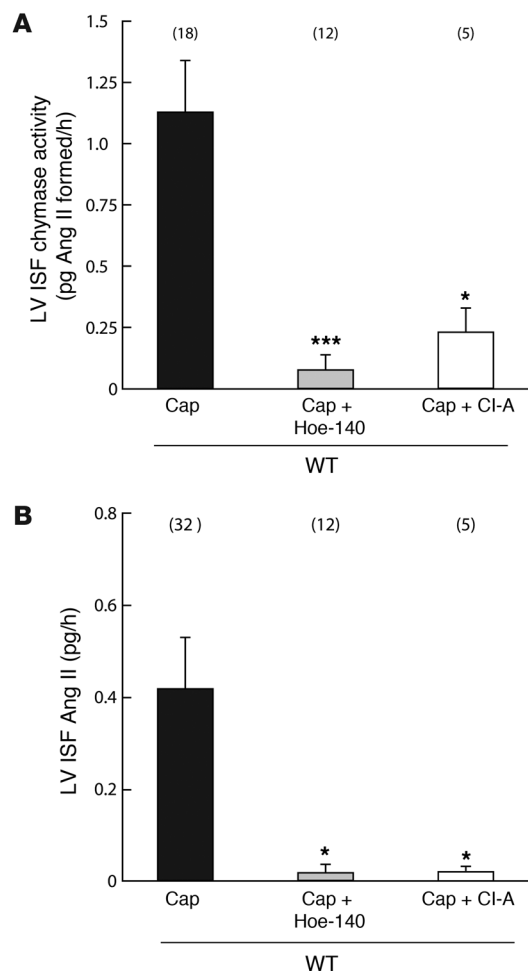
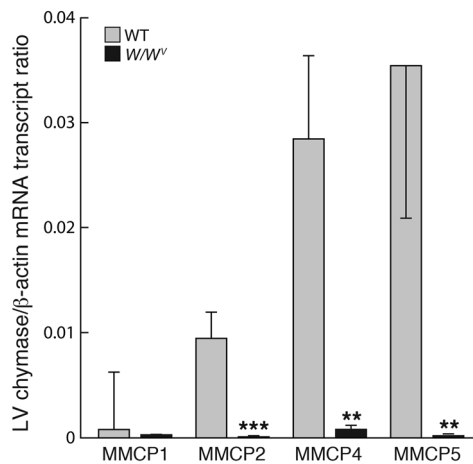


Figure 5
Effect of chronic (2 weeks) ACE inhibition (Captopril, 150 mg/kg/d) on (A) chymase activity and (B) Ang II in the LV ISF on conscious WT mice concurrently treated with vehicle, chymase inhibitor (Cl-A, 200 mg/kg, b.i.d.) (Cl), or bradykinin B2 receptor antagonist (Hoe-140, 0.5 mg/kg/d). Values are mean ± SEM. In each group, values in parentheses represent *n*. * $P < 0.05$; *** $P < 0.001$.

**Figure 6**

β -actin-normalized MMCP1, MMCP2, MMCP4, and MMCP5 mRNA levels in LV tissues from WT and W/W^v mice. Values are mean \pm SEM; $n = 7$ in each group. ** $P < 0.01$; *** $P < 0.001$.

Hoe-140 produced a greater than 10-fold decrease in LV ISF Ang II in chronic ACE-inhibited mice (Figure 5B) ($P < 0.05$).

MMCP4 regulates Ang II in the LV ISF. The mouse genome has multiple chymase genes: MMCP1, -2, -4, -5, -9, -10, and -L (27). Quantitative RT-PCR shows that MMCP4/5 gene expression in the LV was higher than MMCP1/2 gene expression (Figure 6). Other chymase mRNA transcripts could not be detected in the LV. In W/W^v LVs, all chymase mRNA transcripts were undetectable (Figure 6), which suggests that chymases are chiefly elaborated by MCs in the LV.

Purified skin MMCP4 has Ang II-forming activity, but it also degrades Ang II (Supplemental Figure 1, A and B), whereas purified heart MMCP5 does not metabolize Ang I or Ang II (Supplemental Figure 2, A and B) because it is an elastase (Supplemental Figure 2C) (28, 29). Because (a) MMCP4 is a more than 100-fold more efficient Ang II-forming enzyme than MMCP1 or -2 (22) and (b) LV MMCP1 and 2 mRNA transcripts are low abundance (Figure 6), the dominant Ang II-forming chymase in the mouse LV is likely to be MMCP4. To evaluate this, we examined several human chymase inhibitors and found that 4-[1-(4-methyl-benzo[*b*]thiophen-3-yl methyl)-1H-benzimidazol-2-yl sulfanyl]-butyric acid (CI-A) inhibited purified MMCP4 with high affinity ($K_i = 39.7 \pm 1.7$ nM; $n = 4$). Chronic ACE inhibition produced a 14-fold increase in LV ISF chymase activity ($P < 0.01$) (Figure 3F). In these ACE inhibitor-treated WT mice, CI-A treatment (200 mg/kg, b.i.d.) caused a 5-fold ($P < 0.05$) inhibition of LV ISF chymase activity and decreased LV ISF Ang II by 16-fold ($P < 0.05$) (Figure 5, A and B). Moreover, chronic ACE inhibition decreased LV ISF Ang II by $69\% \pm 27\%$ in MC-deficient W/W^v mice ($n = 22$; $P < 0.001$), but not in WT mice (Figure 3B). Taken together, these findings provide evidence that MC MMCP4 release regulates LV ISF Ang II during chronic ACE inhibition.

Chymase limits the efficacy of ACE inhibitor therapy in MI. Here we show that ACE inhibition causes LV MC chymase release, which then activates Ang I. Previous in vitro studies suggest that chymase also activates/inactivates proteins, which could be important in the pathogenesis of cardiac diseases if they occur in vivo (7). Given this, we tested to determine whether chymase limits ACE inhibitor efficacy in the post-MI heart. The adult mouse heart has chymase activity, but a direct Ang II effect on cardiomyocytes in vivo is not

easily demonstrable (30, 31). We chose the hamster as a model system because Ang II-forming chymase activity and chymase-to-ACE activity ratio in hamster heart homogenates is similar to that observed in humans (32) and, as in the human heart (33), Ang II produces a positive inotropic effect in the hamster heart (21, 34).

We tested to determine whether the beneficial effects of ACE inhibitor therapy are limited by chymase in hamsters with MI. Post-MI LV function was analyzed by echocardiography. In hamsters, LV ejection fraction (EF) and fractional shortening (FS) were depressed by 36% ($P < 0.001$) and 50% ($P < 0.001$), respectively, by MI (Figure 7, A and B). In the myocardium, distal to the site of infarction, average cardiomyocyte diameters (Figure 7C) and fibrosis (Figure 7D) were increased by 31% ($P < 0.001$) and 36% ($P < 0.01$), respectively, 35 days after MI. ACE inhibitor therapy (10 mg temocapril/kg/d) started 24 hours after MI and continued for 34 days, improved LV EF and FS by 20% ($P < 0.01$) and 26% ($P < 0.01$), respectively, and decreased infarct size by 26% ($P < 0.001$) (Figure 7, A, B, and E). But MI-induced increase in cardiomyocyte diameter and fibrosis in the noninfarcted LV was not altered by ACE inhibition (Figure 7, C and D). To determine whether potential ACE inhibitor-induced chymase release limits the beneficial effects of ACE inhibitor treatment, we examined the difference in the effect of chymase inhibition in the untreated versus the ACE inhibitor-treated post-MI heart. The hamster has 2 known chymases. Hamster chymase-1, which converts Ang I to Ang II (35), is a homolog of MMCP4 (27), and hamster chymase-2, which does not, is a homolog of MMCP5 (36). We tested and found that 4-[1-(naphthalen-1-yl methyl)-1H-benzimidazol-2-yl sulfanyl]-butyric acid (CI-B) inhibits purified hamster chymase-1 with a K_i of 30.6 ± 3.75 nM ($n = 4$). Compared with vehicle treatment, CI-B (100 mg/kg/d; started 24 hours after MI for 34 days) therapy produced an 18% ($P < 0.001$) decrease in average cardiomyocyte diameter in the noninfarcted LV (Figure 7C) and reduced infarct size by 24% ($P < 0.001$) (Figure 7E). There was a small improvement in LV function, but this change did not reach significance. In contrast, when compared with ACE inhibitor monotherapy, combination therapy (10 mg temocapril/kg/d plus 100 mg CI-B/kg/d; started 24 hours after MI for 34 days) improved LV EF and FS by 16% ($P < 0.05$) and 19% ($P < 0.05$), respectively, and reduced infarct area by 51% ($P < 0.01$) and LV end-diastolic dimension by 24% ($P < 0.05$) (Figure 7, A, B, E, and F). In the distal myocardium, combination therapy, relative to ACE inhibitor monotherapy, reduced MI-induced interstitial fibrosis by 50% ($P < 0.0002$) (Figure 7D) and cardiomyocyte diameters by 18% ($P < 0.001$) (Figure 7C). These beneficial effects were unlikely to be due to differences in hemodynamic effects of ACE/chymase inhibition because mean arterial blood pressures or heart rates in hamsters with MI were unaffected by drug treatments (Supplemental Table 2).

Using Kaplan-Meier survival analysis, we found that post-MI survival was greater in hamsters treated with an ACE and chymase inhibitor combination, relative to vehicle-treated hamsters, than with ACE inhibitor alone (Figure 7G). Remarkably, in the combination therapy group, survival was no different from that observed in sham-operated controls. Together, these findings suggest that ACE inhibitor treatment causes chymase to become an important contributor to cardiac dysfunction and adverse remodeling in the post-MI hamster heart.

Discussion

Here we show that ACE is the key Ang II-forming enzyme in the LV ISF of conscious mice. However, although chronic ACE inhibitor

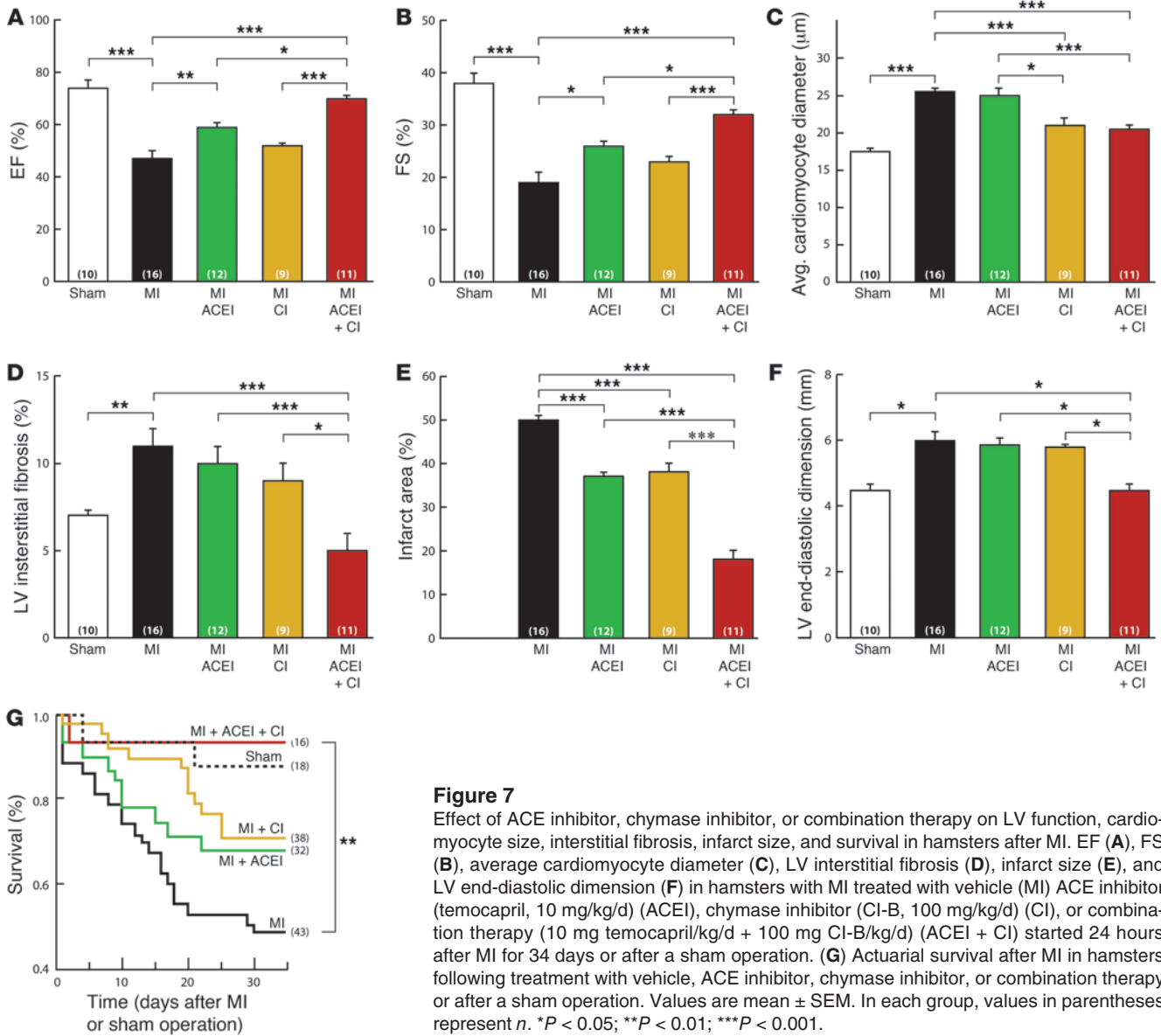


Figure 7

Effect of ACE inhibitor, chymase inhibitor, or combination therapy on LV function, cardiomyocyte size, interstitial fibrosis, infarct size, and survival in hamsters after MI. EF (A), FS (B), average cardiomyocyte diameter (C), LV interstitial fibrosis (D), infarct size (E), and LV end-diastolic dimension (F) in hamsters with MI treated with vehicle (MI) ACE inhibitor (temocapril, 10 mg/kg/d) (ACEI), chymase inhibitor (CI-B, 100 mg/kg/d) (CI), or combination therapy (10 mg temocapril/kg/d + 100 mg CI-B/kg/d) (ACEI + CI) started 24 hours after MI for 34 days or after a sham operation. (G) Actuarial survival after MI in hamsters following treatment with vehicle, ACE inhibitor, chymase inhibitor, or combination therapy or after a sham operation. Values are mean ± SEM. In each group, values in parentheses represent n. *P < 0.05; **P < 0.01; ***P < 0.001.

therapy inhibits ISF ACE activity, it does not lower ISF Ang II levels. This apparent paradox is due to the fact that the chronic ACE inhibitor treatment changes the normal balance of Ang II-forming activity in the LV ISF from being predominantly ACE dependent to being predominantly chymase dependent. The discovery of an ACE inhibitor-induced, chymase-dependent Ang II formation mechanism in the LV raises questions regarding our clinical assumptions about the rationale for using ACE inhibitors in treating cardiac diseases, namely, to suppress Ang II in the heart.

Based on (a) chymase gene expression profiling in the mouse LV, (b) enzyme kinetics with mouse chymases whose genes are highly expressed in the LV, and (c) in vivo conscious mouse studies with a selective chymase substrate ([Pro¹¹,DALa¹²]Ang I) (14) and a specific chymase inhibitor targeted toward the only LV-expressed chymase that has efficient Ang II-forming activity (i.e., MMCP4), we propose that MMCP4 is the enzyme responsible for the non-ACE Ang II-forming activity in the mouse LV.

Our immunohistochemical study shows occurrence of MMCP4-positive MCs in the LV. In addition, we show that in MC-deficient *W/W^v* mice, MMCP4 mRNA is undetectable, non-ACE Ang II-forming activity is undetectable, and ACE inhibitor-dependent increase in LV ISF chymase activity does not occur. Based on these findings, we propose that the MMCP4-positive MC in the mouse LV is the likely source of the non-ACE Ang II-forming activity in the LV ISF. While more extensive adoptive transfer experiments might conceivably strengthen this conclusion, technical limitations make this approach difficult or impossible. Thus, it is possible that non-MC, c-kit-expressing cells in the LV could potentially account for the chymase activity that we detect.

ACE inhibition also decreases bradykinin degradation, which increases ISF bradykinin (24). It is possible that the release of MC chymase in vivo is a direct effect of bradykinin on MCs. This is suggested by our identification of kinin B2 receptors on LV MMCP4-positive MCs as well as the well-established reports that kinin B2

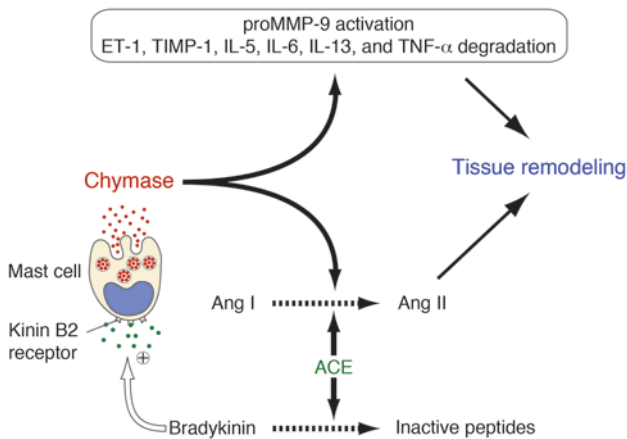


Figure 8

ACE-dependent bradykinin degradation limits baseline secretion of MC chymase in the LV. Chronic inhibition of ACE reduces its direct effects on Ang I to Ang II conversion, but it increases bradykinin/B2 receptor-dependent chymase release from MCs, which counteracts the direct effect of ACE inhibition on Ang II formation through the chymase pathway of Ang II formation. In this scheme, we suggest that the effect of bradykinin on MC chymase release is direct; however, it is also possible that the bradykinin/B2 receptor mechanism indirectly causes chymase release. Chymase release also has a myriad of effects on factors that promote the inflammatory response and tissue remodeling. ET-1, endothelin-1; TIMP-1, tissue inhibitor-1 of metalloproteinase.

receptor activation mobilizes inositol 1,4,5-trisphosphate-evoked Ca^{2+} in several cell types (37) and that increases in intracellular Ca^{2+} or inositol 1,4,5-trisphosphate cause MC degranulation (38). The finding that kinin B2 receptor antagonism prevents ACE inhibitor-dependent release of chymase into the LV ISF supports a role for bradykinin in this process; however, it does not exclude the possibility that the effect is indirect.

The notion that enzymes other than ACE are involved in tissue Ang II generation in vivo has been keenly debated. The basis for this debate revolves around the effect of ACE inhibition on circulating and tissue Ang II levels. On the one hand, it has been shown that tissue Ang II levels are almost completely suppressed by acute ACE inhibition in rodents (39), and plasma Ang II levels are markedly suppressed in hypertensive patients after acute ACE inhibitor therapy (17). On the other hand, chronic ACE inhibitor therapy does not suppress plasma Ang II in hypertensive patients (17). This phenomenon, also known as “ACE inhibitor escape,” has been attributed to incomplete tissue ACE inhibition in the face of elevated plasma Ang I levels (40, 41) or, by some, to a methodological artifact (39). Lack of a mechanistic understanding of this phenomenon and the fact that tissue Ang II is a complex measurement that simultaneously determines Ang II in multiple tissue compartments (e.g., interstitial, cell associated, and intravascular) has impeded the successful resolution of this debate. We show that chymase, although abundant in tissue homogenates, is relatively low in the LV interstitium of conscious mice. Importantly, we also show that chronic ACE inhibition causes a bradykinin-mediated release of MC chymase into the LV ISF. Although ACE inhibition rapidly increases bradykinin levels, its effect on LV interstitial chymase levels may be gradual. MC degranulation with the sequestration of the positively charged chymase by the negatively charged intracellular matrix (10, 42) may be required to elevate interstitial chymase, which then helps to maintain steady-state LV ISF Ang II at pre-ACE inhibition levels — our data suggest that after ACE inhibition is initiated, the increase in ISF chymase levels in the mouse LV may take as little as 24 hours.

Could the benefits of chronic ACE inhibitor use in the treatment of cardiac diseases be limited because of ACE inhibitor-dependent chymase release into the cardiac ISF? Chymase release not only sustains Ang II levels in the heart, but also processes a number of substrates including endothelin-1, pro-MMP-9, and pro-MMP-3 that promote tissue remodeling (Figure 8) (7, 43). We used an orally active chymase inhibitor to directly determine

whether the potential benefits of ACE inhibitor use in MI are limited by chymase. Chronic ACE inhibition improved LV function after MI. Because the beneficial effect of chymase inhibition was greater when combined with ACE inhibition, we conclude that ACE inhibition in the heart causes the release of chymase. LV ISF Ang II and chymase activity could not be measured directly due to difficulties of microdialysis probe insertion in the infarcted heart. But one possibility is that this mechanism limits ACE inhibitor-dependent reduction in LV ISF Ang II by now maintaining LV ISF Ang II at high levels via chymase-dependent Ang II generation. Another possibility is that the effects of chymase on other regulatory proteins (Figure 8) contribute to adverse post-MI LV remodeling and to deterioration of LV function that limits post-MI survival. Thus, for example, chymase inhibition may suppress pro-MMP activation caused by the enzymatic actions of ACE inhibitor-dependent chymase release from MCs. This could explain the more compact and smaller area of scar seen with combination therapy relative to ACE inhibitor therapy alone. Drugs were given 24 hours after left anterior descending artery occlusion. This timing was based on the reported maximal increase in LV free wall ACE and chymase activities that occurs 3 days after MI in hamsters (44). If the initial infarct size was the same but scar formation was improved by chymase inhibitor addition to ACE inhibitor therapy, LV function could improve because of a decrease in LV end-diastolic dimension. We propose that the cardiac benefits of ACE inhibition may be better realized by combining it with simultaneous chymase inhibition. Cardiac diseases, including hypertensive heart disease, viral myocarditis, and atherosclerotic coronary artery disease, the prelude to MI, which are treated with ACE inhibitors, have an inflammatory component that is associated with MC accumulation in the heart (7). This suggests a role for chymase inhibition in improving outcomes for heart disease patients on ACE inhibitor therapy.

Study limitations. In studying the cellular pathway(s) responsible for chymase release, we used the mouse model. Its choice was primarily dictated by the availability of mice with genetic MC deficiency (19) and from analyses that showed equivalent levels of ACE and non-ACE activity in LV homogenates from WT controls of MC-deficient W/W^0 mice (Figure 1). We show that this WT mouse contains a chymase (MMCP4) in the heart that is a net Ang II-forming enzyme. Although there are many similarities in the substrate recognition profiles of human chymase and MMCP4, human chymase differs from MMCP4 in that the latter, but not the former, has apprecia-



ble angiotensinase activity, which allows human chymase to more robustly generate Ang II (6, 28). Thus, studies in the mouse may underestimate the overall contribution of the human MC non-ACE pathway in local cardiac Ang II formation.

The mouse model has a second limitation in that its cardiomyocytes *in vivo* from adult animals are relatively unresponsive to Ang II (30, 31). This led us to choose the hamster for functional studies. In the adult hamster, as with humans, cardiomyocytes are responsive to Ang II (21, 33, 34, 45). Species variability in chymases is striking. Realizing this, we first validated the use of the chymase inhibition strategy in hamsters. We purified hamster chymase 1, a homolog of MMCP4, showed that it is Ang II forming, and identified an orally active high-affinity inhibitor (CI-B) of this enzyme.

The effect(s) of species differences in AT₂ receptor in the heart, which has been shown in some studies to be beneficial (46) and in others to be detrimental (9), could also be a limitation with respect to the implied importance of chymase-based Ang II generation in humans with MI. But the importance of the AT₂ receptor is difficult to “factor in” because its role in the human heart is as yet undefined. Based on these limitations, we realize that the significance of ACE inhibitor-dependent chymase release as a therapeutic target in MI necessarily requires clinical evidence. Nevertheless, the importance of our studies is that they provide an evidence-based hypothesis for a study of the role of cardiac MC chymase in patients that are currently treated with ACE inhibitors. Because ACE inhibitors are some of the most effective and widely used drugs in the treatment of heart diseases, minimizing adverse effects, such as chymase release, has the potential to be highly useful in the treatment of heart failure, let alone other cardiovascular disorders that have an inflammation component.

Methods

Mice. Ten-week-old MC-deficient *W/W^v* mice (background, C57BL/6) (19) and their MC-sufficient WT littermates were purchased from the Jackson Laboratory. All animal studies were approved by the University of Alabama at Birmingham IACUC guidelines for animal care and treatment.

Measurement of ACE and non-ACE Ang II-forming activities in the mouse LV tissue homogenates. LV tissue from WT and *W/W^v* mice was homogenized in 2 ml of 50 mM NaH₂PO₄ buffer, pH 7.4, using a Polytron homogenizer at 9,000 rpm for 15 seconds at 4°C, then centrifuged at 30,000 g for 20 minutes at 4°C and the pellet retained. This procedure was repeated twice. Resulting supernatant fractions, S-1 and S-2, were kept. The pellet was resuspended in 0.5 ml 50 mM NaH₂PO₄ buffer, pH 7.4, containing 100 mM NaCl and 10 mM MgCl₂, and 5 µl of this was added to 35 µl of assay buffer (20 mM Tris-HCl, pH 8.0, containing 0.5 M KCl and 0.01% Triton X-100) containing either no further additive or 10 µM lisinopril and preincubated for 30 minutes at 0°C. Ten microliters of 1 mM Ang I was added to 40 µl of the preincubated aortic extract, and incubations were for 40 minutes at 37°C. Reactions were terminated by the addition of 300 µl ethanol. Precipitated proteins were removed by centrifugation, and the supernatant containing angiotensins was dried. The residue, resuspended in 125 µl of distilled water, was applied to a C₁₈ HPLC column (Vydac); angiotensins were separated as described (22, 27). Total and ACE-independent Ang II-forming activities were determined in duplicate from assays containing either buffer or lisinopril, respectively. ACE-dependent Ang II-forming activity was taken as total minus ACE-independent activity. Assays were optimized to ensure that Ang II generation was linear with time. With crude membrane preparations, positively charged chymases were quantitatively retained in the pellet, as was ACE, which was membrane bound. Ang II-forming activity in S-1 and S-2 was negligible.

Preparation and implantation of microdialysis probes. Microdialysis probes were inserted into the LV myocardium of 10-week-old male *W/W^v* and age-matched WT mice using a modification of a previously described procedure (24). Briefly, each microdialysis probe consisted of a semipermeable membrane fiber (Hospal) with a molecular weight cutoff of 35 kDa (internal diameter = 250 µm) with Pebax tubing (outer diameter = 200 µm) inserted within it and sealed in place at each end of the dialysis fiber such that 4 mm of semipermeable membrane fiber remained exposed at the center of the assembly; this exposed region resided within the LV myocardium free wall. A BV-1 tapered needle with 1-cm length of 7-0 Prolene suture was secured in one end of the probe and a 2-cm length of polyethylene PE-50 tubing was secured to the other end. With animals under general anesthesia (isoflurane, 2%–3%) and using mechanical ventilation, the microdialysis probe was implanted in the LV. An incision was made between the sixth and seventh ribs on the left side, intercostal muscles were cut, and the ribs spread. The heart was thus exposed and the microdialysis probe inserted caudal to rostral in the LV myocardium. The microdialysis probe was fixed in the myocardium such that the dialysis fiber would not work itself out of the LV wall. The Pebax tubing exited the thoracic cavity one intercostal space above and one below the incision. The lungs then were fully inflated, and the sixth and seventh ribs were sutured together. The ends of the probe were transferred subcutaneously to the base of the neck and exteriorized and secured with silicone sealant (Kwik-Cast; World Precision Instruments). After implantation, the probe was perfused with 0.9% saline using a precision infusion syringe pump (BAS) at a flow rate of 0.5 µl/min. The mice were then allowed to recover for 1 day before ISF collections were implemented. At the end of the ISF collection, Evans blue dye was introduced into the probe to visually determine whether the probe was positioned correctly in the LV. The dialysate was collected from the outflow tube in 200 µl Eppendorf tubes containing 10 µl 1 M acetic acid at 0°C. At the end of the collection period, the Eppendorf tubes with their contents were frozen at -80°C.

Mouse experimental protocols. In the first protocol, mice, divided into 3 groups, each group subdivided by the genotypes WT and *W/W^v*, were used for measurement of ISF and plasma Ang I and Ang II concentrations. At day 1, randomized WT and *W/W^v* mice started with vehicle or oral ACE inhibitor-captopril (150 mg/kg/d) treatment. At day 8, microdialysis probe was implanted inside LV myocardium in both genotypes. At day 9, after 24 hours recovery from surgery, ISF dialysate was collected from the microdialysis probes implanted in conscious, nonsedated mice over a 24-hour collection period by infusion of 0.9% saline at a flow rate of 0.5 µl/min; this was used for the measurement of baseline LV ISF Ang II. At day 10, ISF infusion protocol was implemented in WT and *W/W^v* mice for the infusion of ACE-selective ([Pro¹⁰]Ang I) or chymase-selective Ang I ([Pro¹¹,DAla¹²]Ang I) substrates or 0.9% saline at a flow rate of 0.5 µl/min. This protocol allowed the collection of dialysates for (a) baseline ISF Ang I measurement following ISF infusion of 0.9% saline after oral vehicle or captopril treatment for 10 days; (b) ISF Ang II measurement following ISF infusion (0.5 µl/min) of 500 nM [Pro¹¹,DAla¹²]Ang I after vehicle or oral captopril treatment for 10 days; or (c) ISF Ang II measurement following ISF infusion (0.5 µl/min) of 500 nM [Pro¹⁰]Ang I after vehicle or oral captopril treatment for 10 days. These protocols allowed the determination of baseline LV ISF Ang II and Ang I as well as chymase-dependent Ang II-forming activity ([Pro¹¹,DAla¹²]Ang I-dependent Ang II formation – baseline Ang II in the LV ISF) and ACE-dependent Ang II-forming activity ([Pro¹⁰]Ang I-dependent Ang II formation – baseline Ang II in the LV ISF) after 10 days of vehicle treatment or 10 days of ACE inhibitor treatment. Pooled blood samples for measurement of angiotensins in plasma were collected by heart puncture at the time of sacrifice.

In the second protocol, at day 1, WT mice were given either (a) oral captopril treatment (150 mg/kg/d) (mouse group A); (b) oral captopril treatment



(150 mg/kg/d; Sigma-Aldrich) supplemented with the B2 receptor antagonist Hoe-140 (0.5 mg/kg/d; Sigma-Aldrich) (mouse group B); or (c) oral captopril treatment (150 mg/kg/d) supplemented with the chymase inhibitor CI-A (200 mg/kg, b.i.d.; Teijin Pharma Limited) (group C). At day 8, microdialysis probe was implanted inside LV myocardium. At day 9, after 24 hours recovery from surgery, ISF dialysate collection was implemented from the implanted microdialysis probes in conscious, nonsedated mice in groups A–C over a 24-hour collection period during which 0.9% saline was infused at a flow rate of 0.5 μ l/min. This was used for the measurement of baseline LV ISF Ang II during either chronic ACE inhibitor treatment, chronic ACE inhibitor treatment plus B2 receptor blockade, or chronic ACE inhibitor treatment plus chymase inhibitor treatment. Immediately following this, 500 nM [Pro¹¹,DAla¹²]Ang I was infused (0.5 μ l/min) into the microdialysis probe and dialysate was collected over the next 24 hours for the measurement of Ang II in order to calculate LV ISF chymase activity. In these experiments, captopril was prepared in drinking water, CI-A was orally administered by gavage, and Hoe-140 (American Peptide Company) was administered using osmotic minipumps. From the measurement of [Pro¹¹,DAla¹²]Ang I-dependent Ang II formation – baseline Ang II in the LV ISF in each group, we calculated the effects of chronic ACE inhibition (group A), chronic ACE inhibition plus B2 receptor blockade (group B), and chronic ACE inhibition plus chronic chymase inhibition (group C) on LV ISF chymase activity.

Measurements of angiotensins in blood plasma, LV ISF. Angiotensin peptide concentrations were determined using solid-phase extraction, HPLC, and RIA (24).

Immunohistochemistry. Mouse hearts were immersion fixed in 4% paraformaldehyde and stored in 70% ethanol until paraffin embedding and sectioning. Sections (5 μ m) were mounted on slides, deparaffinized in xylene, and placed in ethanol. Tissue sections were treated with the Mouse on Mouse Immunodetection Kit Fluorescein (FMK-2201; Vector Labs) in conjunction with mouse B2 bradykinin receptor mAb (610452, 1:50; BD Transduction Laboratory). Sections were blocked with 5% goat serum in 1% bovine serum for 1 hour at 22°C. Rabbit polyclonal Ab was made against the MMCP4 sequence ETSPVNVIPRPSD; it recognizes a peptide sequence unique to this isoform. The MMCP4 polyclonal Ab (1:100) or ACE polyclonal Ab (1:100; sc20891; Santa Cruz Biotechnology Inc.) in 5% goat serum was applied to sections for 12 hours at 4°C. The sections were incubated with Alexa Fluor 488 (green) or 594 (red) goat anti-mouse or rabbit to visualize the specific stains. Secondary antibodies were from Molecular Probes. Sections were counterstained with DAPI (blue) (Molecular Probes) to reveal nuclei. Image acquisition was performed on a Leica DM6000B epifluorescence microscope (Leica Microsystems) with a Hamamatsu ORCA ER cooled CCD camera and SimplePCI software (Compix Inc.). Images were adjusted appropriately to remove background fluorescence.

Determination of mRNA expression in the mouse LV. For mRNA transcript measurements, mRNA was either extracted from freshly dissected LVs or cardiomyocytes isolated from individual adult mouse hearts (47). Total RNA was extracted with RNAagents (Invitrogen). mRNA was reverse transcribed using Transcriptor reverse transcriptase (Roche) according to the manufacturer's protocols. Real-time PCR reactions were carried out using iCycler and iQ SYBR Green Supermix (Bio-Rad). The primer sets for β -actin, GAPDH, and MMCP1, -2, -4, -5, -9, -10, and -L were as previously reported (22, 47). Forward and reverse mouse ACE PCR primers were 5'-GGGGGCCAAGCTCAAGCAGG-3' and 5'-GCACGTGCCGGTCCAG-GTTC-3', respectively. Real-time PCR conditions for these primers were optimized as 3 mM Mg²⁺, 5 pmol primer, and 50 ng cDNA in a total reaction volume of 25 μ l. The amplifying conditions were determined empirically and were 95°C for 30 seconds, 62°C for 30 seconds (or 59°C for 30 seconds for GAPDH), and 72°C for 60 seconds for 45 cycles. All PCR

products appeared as single bands of the expected molecular size by 1.5% agarose gel fractionation; these PCR products were sequenced to identify target cDNAs. In addition to confirming that all PCR products appeared as a single band of the expected molecular size, we also verified that each PCR product consisted of only a single species, as determined by melting curve analysis. To determine copy number, standard curves for each target transcript were established using purified PCR products. Standard curves were linear and the correlation coefficients were greater than 0.99.

Hamsters. Syrian hamsters, 8 weeks old, were obtained from SLC Japan. The animals were housed in individual cages under controlled conditions of constant temperature and humidity and exposed to a 12-hour dark/12-hour light cycle. The hamsters had free access to drinking water and either a standard chow diet or diet chow containing 0.1% CI-B. All animal studies were approved by the Internal Review Committee of Fukuoka University.

Induction of MI in hamsters. MI was induced by permanent ligation of the left anterior descending coronary artery as previously described (48). Briefly, under pentobarbital (50 mg/kg i.p.) anesthesia, hamsters were intubated and artificially ventilated. After left thoracotomy was performed at the fifth intercostal space, the pericardium was incised and the heart was exteriorized. A 6-0 silk suture was placed around the left coronary artery at the most proximal position. In sham-operated hamsters, the suture was placed beside the coronary artery. The muscle and skin layers were sutured and the thoracic cavity was closed.

Hamster experimental protocol. CI-B (Teijin Pharma Ltd.) was used in studies with hamsters. Its K_i value against hamster chymase-1 was estimated to be approximately 30 nM. In a preliminary experiment, 4 hamsters were given 0.1% CI-B in food for 5 days and blood samples were collected to measure the serum concentration of CI-B. The CI-B concentration was measured by reverse-phase HPLC using a linear gradient (from 0.1% acetic acid containing 0% acetonitrile to 0.1% acetic acid containing 60% acetonitrile). The serum concentration of CI-B was 7.9 ± 2.1 μ M, which was approximately 250-fold higher than its K_i value against hamster chymase. The ACE inhibitor temocapril was provided by Sankyo Co. The dose of temocapril used (10 mg temocapril/kg/d, oral) was based on previously published data.

For hamster studies, a single experienced investigator performed all MI surgeries. Once MI or sham surgery was performed, the hamsters with MI were randomized. The hamster groups were treated according to the following protocol: group 1, sham-operated; group 2, MI without drug intervention; group 3, MI with temocapril (10 mg/kg/d); group 4, MI with 0.1% CI-B in food (100 mg/kg/d); group 5, MI with temocapril (10 mg/kg/d) and 0.1% CI-B in food. Cardiac echocardiography procedures used to obtain the EF, FS, and LV end-diastolic dimension were performed as previously described by us (48). The survival rates for each treatment group were evaluated over 5 weeks of treatment. At the end of the treatment period, hamsters were sacrificed to collect hearts.

Pathological examination of hamster hearts. The hearts were rinsed in ice-cold saline, and the atria and ventricles were separated to measure ventricular weight. They were then cut at the level of the papillary muscles through the short axis. Tissue blocks were fixed in 4% formaldehyde for 48 hours. After dehydration, the sections were embedded in paraffin, and 4- μ m-thick sections were cut. Deparaffinized sections were stained with H&E and Masson's trichrome. After dehydration in 96% ethanol, the sections were mounted. The epicardial circumferential lengths of the infarcted and non-infarcted LV were determined by computerized morphometry. The infarct zone of the LV was measured and presented as a percentage of the entire epicardial circumferential length of the LV. Average myocytes diameter measurements were performed on myocytes in 10 \times 400 fields. To avoid individual myocyte cross sections that were grossly ellipsoid in shape, the ratio of the long and short axis diameters was measured. Measurements in which this ratio exceeded 1.5 were excluded. Average value from each



hamster heart was based on the data from 130 myocytes. Myocyte diameter was determined on an iMac computer using the public domain NIH Image Program. In order to determine fibrosis area, 6 × 200 fields were analyzed in the midwall area of the noninfarcted interventricular septum. Fibrosis area was expressed as the percentage of aniline blue-positive areas in the fields analyzed relative to the total area of the fields analyzed. Measurements were restricted to the interstitial fibrosis; perivascular and endocardial fibrosis were excluded from the measurements.

Purification of mouse and hamster chymases. MMCP4 and MMCP5 were purified from mouse skin and heart, respectively, according to the methods described previously (49, 50). Hamster chymase-1 was purified from the tongue using procedures described previously (6).

Determination of chymase substrate specificities. All synthetic angiotensins were from Bachem California Inc. 30 mM of Ang I, Ang II, [Val⁸]Ang I, and [Val⁸]Ang II were incubated with the purified MMCP4 and MMCP5 in 20 mM Tris-HCl buffer, pH 7.5, containing 0.5 M NaCl, in a total volume of 50 µl at 37°C for 30 minutes (6). Chymase concentrations were adjusted so that less than 30% of the substrate was consumed during the assay. The reactions were terminated by addition of 50 µl ice-cold 0.25% trifluoroacetic acid. 20 µl of the resulting reactions was applied to a BEH C₁₈ reverse-phase HPLC column (100 mm × 1.7 mm i.d.; Waters Corp.), which was developed using 20-minute linear gradients with acetonitrile containing 0.1% trifluoroacetic acid. The elution position of Ang I, Ang II, [Val⁸]Ang I, [Val⁸]Ang II, and Ang I-(5-10) was determined using pure synthetic angiotensin peptides as standards.

Determination of K_i. K_i values for chymase inhibition were determined using Suc-Ala-His-Pro-Phe-pNA or MeOsuc-Ala-Ala-Pro-Val-pNA (Bachem). Enzyme activities were evaluated by measuring p-nitroaniline release from the synthetic substrates. K_i values were determined from plots of enzyme activity versus inhibitor concentration in which inhibitor concentration was corrected by using the K_m and concentration of the substrate (S) used for the competition ($K_i = IC_{50}/(1 + ([S]/K_m))$).

Statistics. All data are presented as mean ± SEM. In some cases, an unpaired Student's *t* test was used for statistical comparisons between the

WT and W/W⁰ groups. Groups were compared statistically using ANOVA, and the significance of differences was determined by the Bonferroni's test. *P* values of less than 0.05 were considered to indicate statistical significance. For differences in mortality, a Kaplan-Meier survival analysis was performed and differences between the groups were tested by a log-rank analysis using the Cox-Mantel test. Hamsters that died within 24 hours after the operation were excluded from the survival-rate analysis.

Acknowledgments

We thank Robert M. Graham for his helpful comments. This study was supported by grants R01HL60707 and R01HL54816 (to L.J. Dell'Italia); R01HL79040 (to A. Husain); a Specialized Centers of Clinically Oriented Research grant in Cardiac Dysfunction from the NIH (P50HL077100); and a Scientist Development grant from the National American Heart Association (0130306N to C.-C. Wei).

Received for publication March 26, 2009, and accepted in revised form January 20, 2010.

Address correspondence to: Hidenori Urata, Department of Cardiovascular Diseases, Fukuoka University Chikushi Hospital, 1-1-1 Zokumyoin, Chikushino 818-8502 Fukuoka, Japan. Phone: 81.92.801.1011; Fax: 81.92.865.2692; E-mail: uratah@fukuoka-u.ac.jp. Or to: Louis J. Dell'Italia, Department of Medicine, Center for Heart Failure Research, University of Alabama at Birmingham, 434 BMR2, 901 19th St. S, Birmingham, AL 35294. Phone: 205.789.0212; Fax: 205.996.2586; E-mail: dell'Italia@physiology.uab.edu. Or to: Ahsan Husain, Division of Cardiology, Emory University, 101 Woodruff Circle, 319 Woodruff Memorial Research Building, Atlanta, GA 30322. Phone: 404.727.8125; Fax: 404.727.3572; E-mail: ahusai2@emory.edu.

Ming Li's present address is: Victor Chang Cardiac Research Institute, Darlinghurst, New South Wales, Australia.

- Corvol P, Eyries M, and Soubrier F. Peptidyl-dipeptidase A/angiotensin I-converting enzyme. In: Barrett AJ, Rawlings ND, Woessner JF, eds. *Handbook of Proteolytic Enzymes*. 2nd ed. New York, NY: Academic Press, Inc. 2004:332-346.
- The SOLVD Investigators. Effect of enalapril on mortality and the development of heart failure in asymptomatic patients with reduced left ventricular ejection fractions. *N Engl J Med*. 1992; 327(10):685-691.
- Pfeffer MA. Left ventricular remodeling after acute myocardial infarction. *Annu Rev Med*. 1995; 46:455-466.
- Borghgi C, Marino P, Zardini P, Magnani B, Colatrina S, Ambrosioni E. Post acute myocardial infarction: the Fosinopril in Acute Myocardial Infarction Study (FAMIS). *Am J Hypertens*. 1997; 10(10 Pt 2):247S-254S.
- Urata H, Healy B, Stewart RW, Bumpus FM, Husain A. Angiotensin II-forming pathways in normal and failing human hearts. *Circ Res*. 1990;66(4):883-890.
- Urata H, Kinoshita A, Misono KS, Bumpus FM, Husain A. Identification of a highly specific chymase as the major angiotensin II-forming enzyme in the human heart. *J Biol Chem*. 1990; 265(36):22348-22357.
- Dell'Italia LJ, Husain A. Dissecting the role of chymase in angiotensin II formation and heart and blood vessel diseases. *Curr Opin Cardiol*. 2002;17(4):374-379.
- Everett AD, Tufro-McReddie A, Fisher A, Gomez RA. Angiotensin receptor regulates cardiac hypertrophy and transforming growth factor-beta 1 expression. *Hypertension*. 1994;23(5):587-592.
- Senbonmatsu T, Ichihara S, Price E Jr, Gaffney FA, Inagami T. Evidence for angiotensin II type 2 receptor-mediated cardiac myocyte enlargement during in vivo pressure overload. *J Clin Invest*. 2000; 106(3):R25-R29.
- Urata H, et al. Cellular localization and regional distribution of an angiotensin II-forming chymase in the heart. *J Clin Invest*. 1993;91(4):1269-1281.
- Singh VP, Le B, Bhat VB, Baker KM, Kumar R. High-glucose-induced regulation of intracellular ANG II synthesis and nuclear redistribution in cardiac myocytes. *Am J Physiol Heart Circ Physiol*. 2007; 293(2):H939-H948.
- Guo C, Ju H, Leung D, Massaeli H, Shi M, Rabinovitch M. A novel vascular smooth muscle chymase is upregulated in hypertensive rats. *J Clin Invest*. 2001; 107(6):703-715.
- Dell'Italia LJ, et al. Compartmentalization of angiotensin II generation in the dog heart. Evidence for independent mechanisms in intravascular and interstitial spaces. *J Clin Invest*. 1997;100(2):253-258.
- Hoit B, Shao Y, Kinoshita A, Gabel M, Husain A, Walsh RA. Effects of angiotensin II generated by an angiotensin converting enzyme-independent pathway on left ventricular performance in the conscious baboon. *J Clin Invest*. 1995;95(4):1519-1527.
- Kokkonen JO, Saarinen J, Kovanen PT. Regulation of local angiotensin II formation in the human heart in the presence of interstitial fluid. Inhibition of chymase by protease inhibitors of interstitial fluid and of angiotensin-converting enzyme by Ang-(1-9) formed by heart carboxypeptidase A-like activity. *Circulation*. 1997;95(6):1455-1463.
- Reilly CF, Tewksbury DA, Schechter NM, Travis J. Rapid conversion of angiotensin I to angiotensin II by neutrophil and mast cell proteinases. *J Biol Chem*. 1982;257(15):8619-8622.
- Biollaz J, Brunner HR, Gavras I, Waeber B, Gavras H. Antihypertensive therapy with MK 421: angiotensin II-renin relationships to evaluate efficacy of converting enzyme blockade. *J Cardiovasc Pharmacol*. 1982;4(6):966-972.
- Mento PF, Wilkes BM. Plasma angiotensins and blood pressure during converting enzyme inhibition. *Hypertension*. 1987;9(6 Pt 2):III42-III48.
- Galli SJ, Kitamura Y. Genetically mast-cell-deficient W/W^v and Sl/Sld mice. Their value for the analysis of the roles of mast cells in biologic responses in vivo. *Am J Pathol*. 1987;127(1):191-198.
- Chattopadhyay S, Karan G, Sen I, Sen GC. A small region in the angiotensin-converting enzyme distal ectodomain is required for cleavage-secretion of the protein at the plasma membrane. *Biochemistry*. 2008;47(32):8335-8341.
- Kinoshita A, Urata H, Bumpus FM, Husain A. Measurement of angiotensin I converting enzyme inhibition in the heart. *Circ Res*. 1993;73(1):51-60.
- Li M, et al. Involvement of chymase-mediated angiotensin II generation in blood pressure regulation. *J Clin Invest*. 2004;114(1):112-120.
- Silver RB, et al. Mast cells: a unique source of renin. *Proc Natl Acad Sci U S A*. 2004;101(37):13607-13612.
- Wei CC, Lucchesi PA, Tallaj J, Bradley WE, Powell PC, Dell'Italia LJ. Cardiac interstitial bradykinin and mast cells modulate pattern of LV remodeling in volume overload in rats. *Am J Physiol Heart Circ*



- Physiol.* 2003;285(2):H784–H792.
25. Joseph K, Kaplan AP. Formation of bradykinin: a major contributor to the innate inflammatory response. *Adv Immunol.* 2005;86:159–208.
 26. Bandeira-Melo C, et al. Suppressive effect of distinct bradykinin B2 receptor antagonist on allergen-evoked exudation and leukocyte infiltration in sensitized rats. *Br J Pharmacol.* 1999;127(2):315–320.
 27. Wouters MA, Liu K, Riek P, Husain A. A despecialization step underlying evolution of a family of serine proteases. *Mol Cell.* 2003;12(2):343–354.
 28. Caughey GH, Raymond WW, Wolters PJ. Angiotensin II generation by mast cell alpha- and beta-chymases. *Biochim Biophys Acta.* 2000;1480(1–2):245–257.
 29. Kunori Y, et al. Rodent alpha-chymases are elastase-like proteases. *Eur J Biochem.* 2002;269(23):5921–5930.
 30. van Kats JP, Methot D, Paradis P, Silversides DW, Reudelhuber TL. Use of a biological peptide pump to study chronic peptide hormone action in transgenic mice. Direct and indirect effects of angiotensin II on the heart. *J Biol Chem.* 2001;276(47):44012–44017.
 31. Reudelhuber TL, Bernstein KE, Delafontaine P. Is angiotensin II a direct mediator of left ventricular hypertrophy? Time for another look. *Hypertension.* 2007;49(6):1196–1201.
 32. Akasu M, Urata H, Kinoshita A, Sasaguri M, Ideishi M, Arakawa K. Differences in tissue angiotensin II-forming pathways by species and organs in vitro. *Hypertension.* 1998;32(3):514–520.
 33. Moravec CS, et al. Inotropic effects of angiotensin II on human cardiac muscle in vitro. *Circulation.* 1990;82(6):1973–1984.
 34. Hirakata H, et al. Angiotensins and the failing heart. Enhanced positive inotropic response to angiotensin I in cardiomyopathic hamster heart in the presence of captopril. *Circ Res.* 1990;66(4):891–899.
 35. Kunori Y, Muroga Y, Iidaka M, Mitsuhashi H, Kamimura T, Fukamizu A. Species differences in angiotensin II generation and degradation by mast cell chymases. *J Recept Signal Transduct Res.* 2005;25(1):35–44.
 36. Kervinen J, et al. Structural basis for elastolytic substrate specificity in rodent alpha-chymases. *J Biol Chem.* 2008;283(1):427–436.
 37. Higashida H, Taketo M, Takahashi H, Yokoyama S, Hashii M. Potential mechanism for bradykinin-activated and inositol tetrakisphosphate-dependent Ca^{2+} influx by Ras and GAP1 in fibroblast cells. *Immunopharmacology.* 1999;45(1–3):7–11.
 38. Tasaka K, Mio M, Okamoto M. The role of intracellular Ca^{2+} in the degranulation of skinned mast cells. *Agents Actions.* 1987;20(3–4):157–160.
 39. Campbell DJ, et al. Effect of reduced angiotensin-converting enzyme gene expression and angiotensin-converting enzyme inhibition on angiotensin and bradykinin peptide levels in mice. *Hypertension.* 2004;43(4):854–859.
 40. Azizi M, Chatellier G, Guyene TT, Murieta-Geofroy D, Menard J. Additive effects of combined angiotensin-converting enzyme inhibition and angiotensin II antagonism on blood pressure and renin release in sodium-depleted normotensives. *Circulation.* 1995;92(4):825–834.
 41. Menard J, Campbell DJ, Azizi M, Gonzales MF. Synergistic effects of ACE inhibition and Ang II antagonism on blood pressure, cardiac weight, and renin in spontaneously hypertensive rats. *Circulation.* 1997;96(9):3072–3078.
 42. Burwen SJ. Recycling of mast cells following degranulation in vitro: an ultrastructural study. *Tissue Cell.* 1982;14(1):125–134.
 43. Caughey GH. Mast cell tryptases and chymases in inflammation and host defense. *Immunol Rev.* 2007;217:141–154.
 44. Jin D, Takai S, Yamada M, Sakaguchi M, Yao Y, Miyazaki M. Possible roles of cardiac chymase after myocardial infarction in hamster hearts. *Jpn J Pharmacol.* 2001;86(2):203–214.
 45. de Gasparo M, Catt KJ, Inagami T, Wright JW, Unger T. International union of pharmacology. XXIII. The angiotensin II receptors. *Pharmacol Rev.* 2000;52(3):415–472.
 46. Kaschina E, et al. Angiotensin II type 2 receptor stimulation: a novel option of therapeutic interference with the renin-angiotensin system in myocardial infarction? *Circulation.* 2008;118(24):2523–2532.
 47. Li M, et al. c-kit is required for cardiomyocyte terminal differentiation. *Circ Res.* 2008;102(6):677–685.
 48. Hoshino F, et al. Chymase inhibitor improves survival in hamsters with myocardial infarction. *J Cardiovasc Pharmacol.* 2003;41(Suppl 1):S11–S18.
 49. Kido H, Fukusen N, Katunuma N. A simple method for purification of chymase from rat tongue and rat peritoneal cells. *Anal Biochem.* 1984;137(2):449–453.
 50. Kunori Y, et al. Rodent alpha-chymases are elastase-like proteases. *Eur J Biochem.* 2002;269(23):5921–5930.